Bose-Einstein Correlations of Charged Pion Pairs in Au + Au Collisions at $\sqrt{s_{NN}} = 200$ GeV

S. S. Adler,[5] S. Afanasiev,[17] C. Aidala,[5] N. N. Ajitanand,[43] Y. Akiba,[20,38] J. Alexander,[43] R. Amirikas,[12] L. Aphecetche,[45] S. H. Aronson,[5] R. Averbeck,[44] T. C. Awes,[35] R. Azmoun,[44] V. Babintsev,[15] A. Baldisseri,[10] K. N. Barish,[6] P. D. Barnes,[27] B. Bassalleck,[33] S. Bathe,[30] S. Batsouli,[9] V. Baublis,[37] A. Bazilevsky,[39,15] S. Belikov,[16,15] Y. Berdnikov,[40] S. Bhagavatula,[16] J. G. Boissevain,[27] H. Borel,[10] S. Borenstein,[25] M. L. Brooks,[27] D. S. Brown,[34] N. Bruner,[33] D. Bucher,[30] H. Buesching,[30] V. Bumazhnov,[15] G. Bunce,[5,39] J. M. Burward-Hoy,[26,44] S. Butsyk,[44] X. Camard,[45] J.-S. Chai,[18] P. Chand,[4] W. C. Chang,[2] S. Chernichenko,[15] C. Y. Chi,[9] J. Chiba,[20] M. Chiu,[9] I. J. Choi,[52] J. Choi,[19] R. K. Choudhury,[4] T. Chujo,[5] V. Cianciolo,[35] Y. Cobigo,[10] B. A. Cole,[9] P. Constantin,[16] D. G. d'Enterria,[45] G. David,[5] H. Delagrange,[45] A. Denisov,[15] A. Deshpande,[39] E. J. Desmond,[5] O. Dietzsch,[41] O. Drapier,[25] A. Drees,[44] R. du Rietz,[29] A. Durum,[15] D. Dutta,[4] Y. V. Efremenko,[35] K. El Chenawi,[49] A. Enokizono,[14] H. En'yo,[38,39] S. Esumi,[48] L. Ewell,[5] D. E. Fields,[33,39] F. Fleuret,[25] S. L. Fokin,[23] B. D. Fox,[39] Z. Fraenkel,[51] J. E. Frantz,[9] A. Franz,[5] A. D. Frawley,[12] S.-Y. Fung,[6] S. Garpman,[29,*] T. K. Ghosh,[49] A. Glenn,[46] G. Gogiberidze,[46] M. Gonin,[25] J. Gosset,[10] Y. Goto,[39] R. Granier de Cassagnac,[25] N. Grau,[16] S. V. Greene,[49] M. Grosse Perdekamp,[39] W. Guryn,[5] H.-Å. Gustafsson,[29] T. Hachiya,[14] J. S. Haggerty,[5] H. Hamagaki,[8] A. G. Hansen,[27] E. P. Hartouni,[26] M. Harvey,[5] R. Hayano,[8] X. He,[13] M. Heffner,[26] T. K. Hemmick,[44] J. M. Heuser,[44] M. Hibino,[50] J. C. Hill,[16] W. Holzmann,[43] K. Homma,[14] B. Hong,[22] A. Hoover,[34] T. Ichihara,[38,39] V. V. Ikonnikov,[23] K. Imai,[24,38] D. Isenhower,[1] M. Ishihara,[38] M. Issah,[43] A. Isupov,[17] B. V. Jacak,[44] W. Y. Jang,[22] Y. Jeong,[19] J. Jia,[44] O. Jinnouchi,[38] B. M. Johnson,[5] S. C. Johnson,[26] K. S. Joo,[31] D. Jouan,[36] S. Kametani,[8,50] N. Kamihara,[47,38] J. H. Kang,[52] S. S. Kapoor,[4] K. Katou,[50] S. Kelly,[9] B. Khachaturov,[51] A. Khanzadeev,[37] J. Kikuchi,[50] D. H. Kim,[31] D. J. Kim,[52] D. W. Kim,[19] E. Kim,[42] G.-B. Kim,[25] H. J. Kim,[52] E. Kistenev,[5] A. Kiyomichi,[48] K. Kiyoyama,[32] C. Klein-Boesing,[30] H. Kobayashi,[38,39] L. Kochenda,[37] V. Kochetkov,[15] D. Koehler,[33] T. Kohama,[14] M. Kopytine,[44] D. Kotchetkov,[6] A. Kozlov,[51] P. J. Kroon,[5] C. H. Kuberg,[1,27] K. Kurita,[39] Y. Kuroki,[48] M. J. Kweon,[22] Y. Kwon,[52] G. S. Kyle,[34] R. Lacey,[43] V. Ladygin,[17] J. G. Lajoie,[16] A. Lebedev,[16,23] S. Leckey,[44] D. M. Lee,[27] S. Lee,[19] M. J. Leitch,[27] X. H. Li,[6] H. Lim,[42] A. Litvinenko,[17] M. X. Liu,[27] Y. Liu,[36] C. F. Maguire,[49] Y. I. Makdisi,[5] A. Malakhov,[17] V. I. Manko,[23] Y. Mao,[7,38] G. Martinez,[45] M. D. Marx,[44] H. Masui,[48] F. Matathias,[44] T. Matsumoto,[8,50] P. L. McGaughey,[27] E. Melnikov,[15] F. Messer,[44] Y. Miake,[48] J. Milan,[43] T. E. Miller,[49] A. Milov,[44,51] S. Mioduszewski,[5] R. E. Mischke,[27] G. C. Mishra,[13] J. T. Mitchell,[5] A. K. Mohanty,[4] D. P. Morrison,[5] J. M. Moss,[27] F. Mühlbacher,[44] D. Mukhopadhyay,[51] M. Muniruzzaman,[6] J. Murata,[38,39] S. Nagamiya,[20] J. L. Nagle,[9] T. Nakamura,[14] B. K. Nandi,[6] M. Nara,[48] J. Newby,[46] P. Nilsson,[29] A. S. Nyanin,[23] J. Nystrand,[29] E. O'Brien,[5] C. A. Ogilvie,[16] H. Ohnishi,[5,38] I. D. Ojha,[49,3] K. Okada,[38] M. Ono,[48] V. Onuchin,[15] A. Oskarsson,[29] I. Otterlund,[29] K. Oyama,[8] K. Ozawa,[8] D. Pal,[51] A. P. T. Palounek,[27] V. S. Pantuev,[44] V. Papavassiliou,[34] J. Park,[42] A. Parmar,[33] S. F. Pate,[34] T. Peitzmann,[30] J.-C. Peng,[27] V. Peresedov,[17] C. Pinkenburg,[5] R. P. Pisani,[5] F. Plasil,[35] M. L. Purschke,[5] A. K. Purwar,[44] J. Rak,[16] I. Ravinovich,[51] K. F. Read,[35,46] M. Reuter,[44] K. Reygers,[30] V. Riabov,[37,40] Y. Riabov,[37] G. Roche,[28] A. Romana,[25] M. Rosati,[16] P. Rosnet,[28] S. S. Ryu,[52] M. E. Sadler,[1] N. Saito,[38,39] T. Sakaguchi,[8,50] M. Sakai,[32] S. Sakai,[48] V. Samsonov,[37] L. Sanfratello,[33] R. Santo,[30] H. D. Sato,[24,38] S. Sato,[5,48] S. Sawada,[20] Y. Schutz,[45] V. Semenov,[15] R. Seto,[6] M. R. Shaw,[1,27] T. K. Shea,[5] T.-A. Shibata,[47,38] K. Shigaki,[14,20] T. Shiina,[27] C. L. Silva,[41] D. Silvermyr,[27,29] K. S. Sim,[22] C. P. Singh,[3] V. Singh,[3] M. Sivertz,[5] A. Soldatov,[15] R. A. Soltz,[26] W. E. Sondheim,[27] S. P. Sorensen,[46] I. V. Sourikova,[5] F. Staley,[10] P. W. Stankus,[35] E. Stenlund,[29] M. Stepanov,[34] A. Ster,[21] S. P. Stoll,[5] T. Sugitate,[14] J. P. Sullivan,[27] E. M. Takagui,[41] A. Taketani,[38,39] M. Tamai,[50] K. H. Tanaka,[20] Y. Tanaka,[32] K. Tanida,[38] M. J. Tannenbaum,[5] P. Tarján,[11] J. D. Tepe,[1,27] T. L. Thomas,[33] J. Tojo,[24,38] H. Torii,[24,38] R. S. Towell,[1] I. Tserruya,[51] H. Tsuruoka,[48] S. K. Tuli,[3] H. Tydesjö,[29] N. Tyurin,[15] H. W. van Hecke,[27] J. Velkovska,[5,44] M. Velkovsky,[44] L. Villatte,[46] A. A. Vinogradov,[23] M. A. Volkov,[23] E. Vznuzdaev,[37] X. R. Wang,[13] Y. Watanabe,[38,39] S. N. White,[5] F. K. Wohn,[16] C. L. Woody,[5] W. Xie,[6] Y. Yang,[7] A. Yanovich,[15] S. Yokkaichi,[38,39] G. R. Young,[35] I. E. Yushmanov,[23] W. A. Zajc,[9,†] C. Zhang,[9] S. Zhou,[7] S. J. Zhou,[51] and L. Zolin[17]

(PHENIX Collaboration)

[1]*Abilene Christian University, Abilene, Texas 79699, USA*
[2]*Institute of Physics, Academia Sinica, Taipei 11529, Taiwan*
[3]*Department of Physics, Banaras Hindu University, Varanasi 221005, India*
[4]*Bhabha Atomic Research Centre, Bombay 400 085, India*

 0031-9007/04/93(15)/152302(6)$22.50

[5]Brookhaven National Laboratory, Upton, New York 11973-5000, USA
[6]University of California–Riverside, Riverside, California 92521, USA
[7]China Institute of Atomic Energy (CIAE), Beijing, People's Republic of China
[8]Center for Nuclear Study, Graduate School of Science, University of Tokyo, 7-3-1 Hongo, Bunkyo, Tokyo 113-0033, Japan
[9]Columbia University, New York, New York 10027 and Nevis Laboratories, Irvington, New York 10533, USA
[10]Dapnia, CEA Saclay, F-91191, Gif-sur-Yvette, France
[11]Debrecen University, H-4010 Debrecen, Egyetem tér 1, Hungary
[12]Florida State University, Tallahassee, Florida 32306, USA
[13]Georgia State University, Atlanta, Georgia 30303, USA
[14]Hiroshima University, Kagamiyama, Higashi-Hiroshima 739-8526, Japan
[15]Institute for High Energy Physics (IHEP), Protvino, Russia
[16]Iowa State University, Ames, Iowa 50011, USA
[17]Joint Institute for Nuclear Research, 141980 Dubna, Moscow Region, Russia
[18]KAERI, Cyclotron Application Laboratory, Seoul, South Korea
[19]Kangnung National University, Kangnung 210-702, South Korea
[20]KEK, High Energy Accelerator Research Organization, Tsukuba-shi, Ibaraki-ken 305-0801, Japan
[21]KFKI Research Institute for Particle and Nuclear Physics (RMKI), H-1525 Budapest 114, POBox 49, Hungary
[22]Korea University, Seoul, 136-701, Korea
[23]Russian Research Center "Kurchatov Institute," Moscow, Russia
[24]Kyoto University, Kyoto 606, Japan
[25]Laboratoire Leprince-Ringuet, Ecole Polytechnique, CNRS-IN2P3, Route de Saclay, F-91128, Palaiseau, France
[26]Lawrence Livermore National Laboratory, Livermore, California 94550, USA
[27]Los Alamos National Laboratory, Los Alamos, New Mexico 87545, USA
[28]LPC, Université Blaise Pascal, CNRS-IN2P3, Clermont-Fd, 63177 Aubiere Cedex, France
[29]Department of Physics, Lund University, Box 118, SE-221 00 Lund, Sweden
[30]Institut für Kernphysik, University of Muenster, D-48149 Muenster, Germany
[31]Myongji University, Yongin, Kyonggido 449-728, Korea
[32]Nagasaki Institute of Applied Science, Nagasaki-shi, Nagasaki 851-0193, Japan
[33]University of New Mexico, Albuquerque, New Mexico, USA
[34]New Mexico State University, Las Cruces, New Mexico 88003, USA
[35]Oak Ridge National Laboratory, Oak Ridge, Tennessee 37831, USA
[36]IPN-Orsay, Universite Paris Sud, CNRS-IN2P3, BP1, F-91406, Orsay, France
[37]PNPI, Petersburg Nuclear Physics Institute, Gatchina, Russia
[38]RIKEN (The Institute of Physical and Chemical Research), Wako, Saitama 351-0198, Japan
[39]RIKEN BNL Research Center, Brookhaven National Laboratory, Upton, New York 11973-5000, USA
[40]St. Petersburg State Technical University, St. Petersburg, Russia
[41]Universidade de São Paulo, Instituto de Física, Caixa Postal 66318, São Paulo CEP05315-970, Brazil
[42]System Electronics Laboratory, Seoul National University, Seoul, South Korea
[43]Chemistry Department, Stony Brook University, SUNY, Stony Brook, New York 11794-3400, USA
[44]Department of Physics and Astronomy, Stony Brook University, SUNY, Stony Brook, New York 11794, USA
[45]SUBATECH (Ecole des Mines de Nantes, CNRS-IN2P3, Université de Nantes), BP 20722, 44307, Nantes, France
[46]University of Tennessee, Knoxville, Tennessee 37996, USA
[47]Department of Physics, Tokyo Institute of Technology, Tokyo, 152-8551, Japan
[48]Institute of Physics, University of Tsukuba, Tsukuba, Ibaraki 305, Japan
[49]Vanderbilt University, Nashville, Tennessee 37235, USA
[50]Waseda University, Advanced Research Institute for Science and Engineering, 17 Kikui-cho, Shinjuku-ku, Tokyo 162-0044, Japan
[51]Weizmann Institute, Rehovot 76100, Israel
[52]Yonsei University, IPAP, Seoul 120-749, Korea

(Received 5 January 2004; published 8 October 2004)

Bose-Einstein correlations of identically charged pion pairs were measured by the PHENIX experiment at midrapidity in Au + Au collisions at $\sqrt{s_{NN}} = 200$ GeV. The Bertsch-Pratt radius parameters were determined as a function of the transverse momentum of the pair and as a function of the centrality of the collision. Using the standard core-halo partial Coulomb fits, and a new parametrization which constrains the Coulomb fraction as determined from the unlike-sign pion correlation, the ratio $R_{\mathrm{out}}/R_{\mathrm{side}}$ is within 0.8–1.1 for $0.25 < \langle k_{\mathrm{T}} \rangle < 1.2$ GeV/c. The centrality dependence of all radii is well described by a linear scaling in $N_{\mathrm{part}}^{1/3}$, and $R_{\mathrm{out}}/R_{\mathrm{side}}$ for $\langle k_{\mathrm{T}} \rangle \sim 0.45$ GeV/c is approximately constant at unity as a function of centrality.

DOI: 10.1103/PhysRevLett.93.152302 PACS numbers: 25.75.Gz, 25.75.Dw

Following its application in the study of proton-antiproton annihilations [1], the study of Bose-Einstein correlations has been used extensively to measure source distributions in relativistic heavy ion collisions [2,3]. These measurements were originally motivated by theoretical predictions of a large source size and/or a long duration of particle emission [4–6] which would result from a softening of the equation of state in a first-order phase transition to a quark-gluon plasma (QGP). The technique of Bose-Einstein correlations is based upon quantum statistical interference, but final state interactions such as Coulomb repulsion modify the relative momentum distributions for pairs of identical particles emanating from the collision region. Both effects are included in multidimensional Gaussian fits to the normalized relative momentum distributions yielding fit parameters which are the rms widths in each dimension, R_{long}, R_{side}, R_{out} [7,8], also referred to as HBT radii to honor the radio astronomers Hanbury Brown and Twiss who pioneered a similar technique to determine the angular diameters of stars [9]. For dynamic (i.e., expanding) sources, the HBT radii depend on the mean transverse momentum of the particle pairs, $k_{\mathrm{T}} = (\mathbf{p}_{1\mathrm{T}} + \mathbf{p}_{2\mathrm{T}})/2$, and correspond to lengths of homogeneity, regions of the source which emit particles of similar momentum [10]. Measuring the k_{T} dependence of the HBT radii provides essential constraints on dynamical models that include the space-time evolution of the source [11,12].

Most hydrodynamical models for the space-time evolution of a rehadronizing QGP predicted that the measurement of the $R_{\mathrm{out}}/R_{\mathrm{side}}$ ratio at moderate values of k_{T} provides a sensitive measure of the expected long duration of particle emission, a signal of a slowly burning first-order phase transition from QGP to hadrons at the Relativistic Heavy Ion Collider (RHIC) [4]. Predictions that the $R_{\mathrm{out}}/R_{\mathrm{side}}$ ratio should reach ~ 1.5 at k_{T} of ~ 0.5 GeV/c were not borne out by initial measurements of Bose-Einstein correlations of pions from Au + Au collisions at $\sqrt{s_{NN}} = 130$ GeV [13,14]. Disagreement between theory and data is known as the "RHIC HBT puzzle" [15].

We present here data on Bose-Einstein correlations of charged pion pairs measured by the PHENIX experiment at RHIC for Au + Au collisions at $\sqrt{s_{NN}} = 200$ GeV. In this analysis, we adopt a recent fitting technique that provides for a self-consistent treatment of the Coulomb final state interaction for a source that is made up of a smaller core and a more extended halo of long-lived resonances. We introduce a new parametrization in which the strength of the Coulomb interaction is constrained by the measured unlike-sign pion correlation.

The PHENIX detector provides particle identification (PID) capabilities for hadrons, leptons, and photons over a wide momentum range. The setup of the PHENIX detector has been described in detail elsewhere [16]. In this analysis, we use the west arm of the central spectrometer, which covers the pseudorapidity region $|\eta| < 0.35$ and $\Delta\phi = \pi/2$ in an azimuthal angle over a region of $0.2 < k_{\mathrm{T}} < 2.0$ GeV/c. The drift chamber (DC), at a radial distance between 2.0 and 2.4 m, provides trajectory information in the azimuthal direction. A pad chamber (PC1) at 2.5 m provides z-coordinate information. Combining the DC and PC1 information, a track model provides a three-dimensional trajectory and momentum vector for charged particles. The momentum resolution is $\delta p/p \simeq 0.7\% \oplus 1.0\% \times p$ (GeV/c), where the first term is due to the multiple scattering before the DC, and the second term results from the angular resolution of the DC. For this analysis, the electromagnetic calorimeter (EMCal) provides the time of arrival of particles at its front face located 5.1 m from the beam axis. The timing resolution is approximately 400 psec for hadrons. This analysis is based on a sample of 34×10^6 minimum-bias events taken with an integrated magnetic field of 0.78 T m and triggered by the coincidence of the beam-beam counters (BBCs) and zero-degree calorimeters (ZDCs)—corresponding to $92\% \pm 2\%$ of the total inelastic cross section of 6.8 b. Event centrality is determined using a correlation measurement between neutral energy deposited in the ZDCs and fast particles recorded in the BBCs [17]. A Monte Carlo Glauber model [18,19] is used with a simulation of the BBC and ZDC responses to determine the number of nucleons participating in the collisions (N_{part}) for the minimum-bias events. About 23×10^6 events are selected with a requirement that the collision vertex position measured by the BBC is within ± 30 cm from the center of the spectrometer. Each track is required to have an associated hit on the EMCal within 2σ of the track's projection to the EMCal, where σ refers to the resolution of the projection. Charged particles are identified by the time-of-flight technique using timing information between the BBC and the EMCal, combined with momentum and path length calculated by the track model. Charged particles in the PID zone within 1.5σ of the ideal squared-mass peak of pions but 1.5σ away from the kaon bands are identified as pions. After the track quality and PID cuts, $\sim 45 \times 10^6$ positive pions and $\sim 51 \times 10^6$ negative pions are selected in a momentum range from 0.2 to 2.0 GeV/c.

The pion correlation function is experimentally defined as $C_2(\mathbf{q}) = A(\mathbf{q})/B(\mathbf{q})$, where $A(\mathbf{q})$ is the measured two-pion (actual pair) distribution of pair momentum difference $\mathbf{q}$, and $B(\mathbf{q})$ is the background pair (mixed pair) distribution generated using mixed events from the same data sample. Event mixing is done selecting events that have similar multiplicities and event vertices. We remove ghost tracks and inefficiencies by removing pairs of tracks in three regions at the drift chambers: $\Delta Z_{\mathrm{DC}} < 1$ cm and $\Delta\phi_{\mathrm{DC}} < 60$ mr, $\Delta Z_{\mathrm{DC}} < 5$ cm and

$\Delta\phi_{\rm DC} < 30$ mr, and $\Delta\phi_{\rm DC} < 5$ mr. We also remove hits affected by EMCal cluster sharing by eliminating tracks with hits separated by less than 8 cm at the EMCal. The event-mixed background pairs are subjected to the same cuts. After pair cuts, $\sim 110 \times 10^6$ positive and 140×10^6 negative pion pairs remain, approximately 40 times the data sample acquired by PHENIX at $\sqrt{s_{NN}} = 130$ GeV [13]. Remaining inefficiencies in the DC and EMCal are small, and for these we apply a correction from a GEANT-based [20] Monte Carlo simulation of the detector. The multiplicity dependence is estimated by embedding simulated pion pairs into real events. The systematic errors from pair cuts and corrections are estimated to be $\sim 4\%$ for $R_{\rm side}$ and $R_{\rm long}$, and $\sim 8\%$ for $R_{\rm out}$. Systematic errors for the Coulomb correction (discussed below) are $\sim 2\%$, and we assign an additional systematic error of 1% to each radius for the so-called residual HBT effect [21] in the event-mixed background. All systematic errors are determined as a function of $k_{\rm T}$ and centrality.

To compare directly to previous analyses, we fit the correlations using a standard *full* Coulomb correction, in which the Coulomb correction is determined iteratively by calculating the Coulomb wave function [6] for a 3D Gaussian parametrization of the source using the radius fit parameters from the previous iteration. We fit the Bose-Einstein correlation with the *full* Coulomb correction to the 1D $q_{\rm inv}$ parametrization, $C_2^{\rm FC}(q_{\rm inv}) = 1 + \lambda_{\rm inv} \times \exp(-R_{\rm inv}^2 q_{\rm inv}^2)$, and the 3D Bertsch-Pratt parametrization is given by

$$C_2^{\rm FC} = 1 + \lambda \exp(-R_{\rm side}^2 q_{\rm side}^2 - R_{\rm out}^2 q_{\rm out}^2 - R_{\rm long}^2 q_{\rm long}^2). \quad (1)$$

The relative momentum $\mathbf{q}$ is decomposed into $q_{\rm side}$, $q_{\rm out}$, and $q_{\rm long}$, where the longitudinal component ($q_{\rm long}$) is parallel to the beam axis, the out component ($q_{\rm out}$) is parallel to the mean transverse momentum of the pair, $\mathbf{k}_{\rm T}$, and the side component ($q_{\rm side}$) is perpendicular to both $q_{\rm long}$ and $q_{\rm out}$ [7,8]. Analysis is performed in the longitudinal center-of-mass system (LCMS), where the mean longitudinal momentum of the pair vanishes. In this frame, the duration of particle emission couples exclusively to $q_{\rm out}$. Cross terms may appear in Eq. (1), but they vanish in our measurement of central collisions at midrapidity for symmetry reasons [22].

In the core-halo model of the source many relatively long-lived particles (e.g., η, η') decay into pions too far from the core to be experimentally resolved by Bose-Einstein interference [23]. These pions also have Coulomb interactions that are negligible. To account for this effect, and to assess the systematic errors that arise from making a clean distinction between the core and halo components of the source, we perform two fits to the correlation function using Eqs. (2) and (3):

$$C_2^{\rm raw} = C_{\rm core} + C_{\rm halo} = [\lambda(1 + G)F] + [1 - \lambda], \quad (2)$$

$$C_2^{\rm raw} = [\lambda(1 + G)F] + [(\lambda_{+-} - \lambda)F] + [1 - \lambda_{+-}], \quad (3)$$

where G corresponds to the Gaussian term in Eq. (1). In Eq. (2) [24–26], the fit is applied to the correlation function without Coulomb correction ($C_2^{\rm raw}$), and the Coulomb correction term F is included in the fit function itself. In Eq. (3) we introduce a new parameter, λ_{+-}, to decouple the Coulomb and Bose-Einstein fractions. This form extends the formalism to allow for intermediate range decay pions, such as from the ω, which may contribute to the Coulomb strength without being resolved in the measured Bose-Einstein correlation [27]. λ_{+-} is determined by fitting Coulomb correlation functions calculated with several Coulomb strengths, assuming the 1D HBT radius obtained from the like-sign pion data, to the unlike-sign correlation function in the range $0.2 < k_{\rm T} < 2.0$ GeV/c, as shown in Fig. 1(a). The test yields a value of Coulomb strength $\lambda_{+-} = 0.50 \pm 0.04$, where χ^2 of the fit becomes minimum (χ^2/d.o.f. $= 32.9/11$).

Figures 1(b)–1(d) show fits to the $\pi^-\pi^-$ correlation functions for the full [Eq. (1)] and partial [Eq. (2)] Coulomb corrections. Figure 2 shows the fit parameters most affected by the strength of the Coulomb correction, and the physically interesting ratio $R_{\rm out}/R_{\rm side}$ for the full Coulomb correction and two types of partial Coulomb corrections. The partial Coulomb correction leads to a reduction in λ at low $k_{\rm T}$ and increases in $R_{\rm out}$ and $R_{\rm out}/R_{\rm side}$, which are most prominent at intermediate $k_{\rm T}$. In all subsequent results, Eq. (2) is used exclusively, and

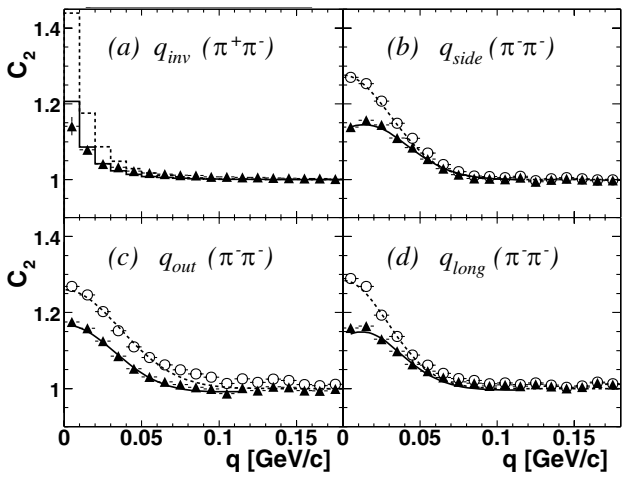

FIG. 1. (a) The one-dimensional correlation function of unlike-sign pions for $0.2 < k_{\rm T} < 2.0$ GeV/c. The two overlaid histograms show calculations for the *full* (dashed) and the 50% partial (solid) Coulomb corrections. (b)–(d) The three-dimensional $\pi^-\pi^-$ correlation function slices for $0.2 < k_{\rm T} < 2.0$ GeV/c and 0%–30% centrality averaged over the lowest 40 MeV/c in the orthogonal directions. The full Coulomb corrected data (open circles) are fit to Eq. (1) (dashed lines), and the data without Coulomb correction (filled triangles) are fit to Eq. (2) (solid lines).

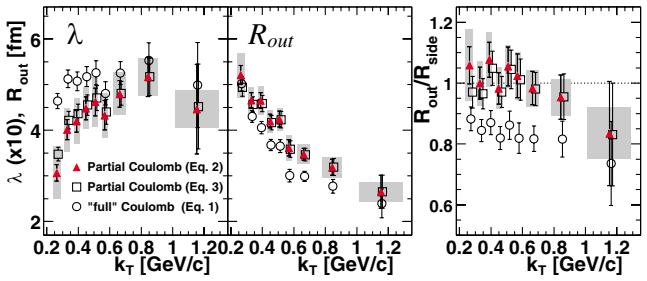

FIG. 2 (color online). The k_T dependence of λ, R_{out}, and R_{out}/R_{side} for $\pi^-\pi^-$ for 0%–30% centrality. Filled triangles show the results from fits to a core-halo structure by Eq. (2), with statistical error bars and systematic error bands. Open circles and squares show the results from the *full* and partial Coulomb corrections by Eqs. (1) and (3), respectively, with statistical error bars.

differences arising from the use of Eq. (3) are incorporated into the total systematic errors.

Figure 3 shows the k_T dependence of all radii and the ratio R_{out}/R_{side}, along with the recently published STAR results [28], and the radii from hydrodynamical model calculations of Hirano [29] and Soff [30]. The results of PHENIX and STAR are in excellent agreement, and reveal in great detail the characteristic ~50% overprediction of these models in R_{out}/R_{side}. The k_T dependence of these radii is reproduced by parametrizations of hydrodynamic freeze-out hypersurfaces [31–33] that are fit to previously published data.

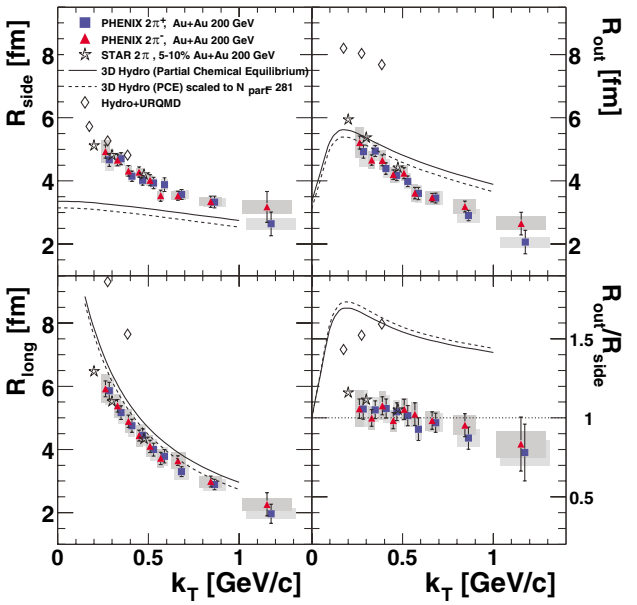

FIG. 3 (color online). The k_T dependence of the Bertsch-Pratt parameters for $\pi^+\pi^+$ (blue square) and $\pi^-\pi^-$ (red triangle) for 0%–30% centrality, from fits to a core-halo structure by Eq. (2), with statistical error bars and systematic error bands. Results from STAR [28] and hydrodynamics models (Hirano [29], solid and dashed lines, and Soff [30], diamonds) are overlaid.

Figure 4 shows that the centrality dependency is well described by a linear function of $N_{part}^{1/3}$. The slope parameters for R_{side} and R_{out} are similar to those measured at 11.6 and 14.6A GeV/c [34], while R_{long} is significantly larger. Therefore the approximate independence of R_{side} and R_{out}, and the increase in R_{long} with $\sqrt{s_{NN}}$ documented in Fig. 2 of [13], can be extended to peripheral collisions as well.

In conclusion, we have presented the Bertsch-Pratt HBT radii in the LCMS for identified charged pions measured by PHENIX in Au + Au collisions at $\sqrt{s_{NN}} = 200$ GeV. The k_T dependence of the HBT radii was measured for $\langle N_{part}\rangle = 281$, and the centrality dependence was measured for $\langle k_T\rangle \sim 0.45$ GeV/c. We performed two different partial Coulomb analyses: one based upon a self-consistent treatment of the Coulomb correction, and the other based upon direct comparison to the unlike-sign correlations. The methods give different results for λ, R_{out}, and R_{out}/R_{side} from those of the full Coulomb correction. Using the partial Coulomb correction of Eq. (2), we observe that the value of R_{out}/R_{side}, as a function of k_T, decreases from ~1.1 to ~0.8 over the range of $k_T = 0.2$–1.2 GeV/c for $\langle N_{part}\rangle = 281$. This ratio remains approximately constant at unity when plotted as a function of the number of participants for $\langle k_T\rangle \sim 0.45$ GeV/c. These measurements are consistent with recent results from STAR for the same system, but they

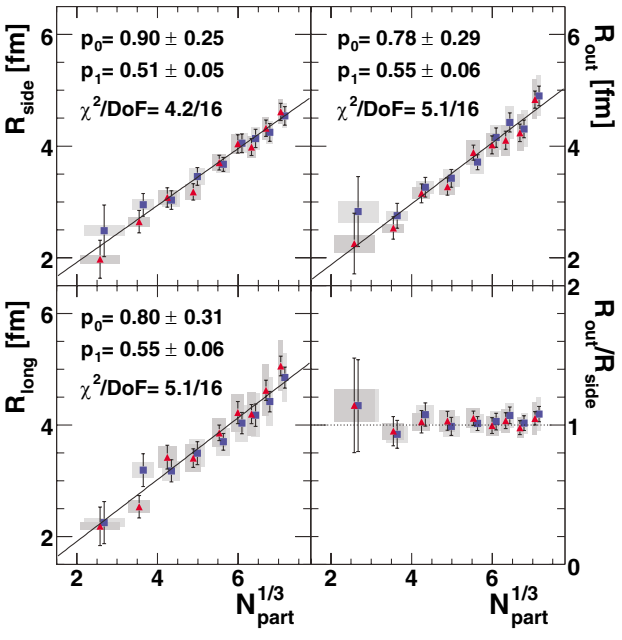

FIG. 4 (color online). Bertsch-Pratt radius parameters versus the cube root of the number of participants ($N_{part}^{1/3}$) for $\pi^+\pi^+$ (blue square) and $\pi^-\pi^-$ (red triangle) for the fits to a core-halo structure by Eq. (2) with statistical error bars and systematic error bands, in the $0.2 < k_T < 2.0$ GeV/c range, with $\langle k_T\rangle \sim 0.45$ GeV/c. The solid line shows fits to $p_0 + p_1 * N_{part}^{1/3}$ for both signs.

are inconsistent with recent hydrodynamical calculations assuming the first-order phase transition from QGP to hadrons. These detailed measurements of the transverse momentum dependence of the HBT radii, in particular, that of $R_{\mathrm{out}}/R_{\mathrm{side}}$, provide extremely strong constraints for models of particle production at RHIC.

We thank the staff of the Collider-Accelerator and Physics Departments at BNL for their vital contributions. We acknowledge support from the Department of Energy and NSF (USA), MEXT and JSPS (Japan), CNPq and FAPESP (Brazil), NSFC (China), CNRS-IN2P3 and CEA (France), BMBF, DAAD, and AvH (Germany), OTKA (Hungary), DAE and DST (India), ISF (Israel), KRF and CHEP (Korea), RMIST, RAS, and RMAE (Russia), VR and KAW (Sweden), U.S. CRDF for the FSU, U.S.-Hungarian NSF-OTKA-MTA, and U.S.-Israel BSF.

*Deceased.
†PHENIX Spokesperson.
Electronic address: zajc@nevis.columbia.edu

[1] G. Goldhaber *et al.*, Phys. Rev. **120**, 300 (1960).
[2] U. A. Wiedemann and U. Heinz, Phys. Rep. **319**, 145 (1999).
[3] T. Csörgő, Heavy Ion Phys. **15**, 1 (2002).
[4] D. H. Rischke and M. Gyulassy, Nucl. Phys. **A597**, 701 (1996).
[5] G. F. Bertsch, Nucl. Phys. **A498**, 173 (1989).
[6] S. Pratt, Phys. Rev. D **33**, 72 (1986).
[7] S. Pratt, Phys. Rev. Lett. **53**, 1219 (1984).
[8] G. Bertsch and G. E. Brown, Phys. Rev. C **40**, 1830 (1989).
[9] R. Hanbury Brown and R. Twiss, Philos. Mag. **45**, 663 (1954).
[10] A. Makhlin and Yu. M. Sinyukov, Z. Phys. C **39**, 69 (1988).
[11] S. Pratt, T. Csörgő, and J. Zimányi, Phys. Rev. C **42**, 2646 (1990).
[12] D. E. Fields *et al.*, Phys. Rev. C **52**, 986 (1995).
[13] K. Adcox *et al.*, Phys. Rev. Lett. **88**, 192302 (2002).
[14] C. Adler *et al.*, Phys. Rev. Lett. **87**, 082301 (2001).
[15] M. Gyulassy, Lect. Notes Phys. **583**, 37 (2002).
[16] K. Adcox *et al.*, Nucl. Instrum. Methods Phys. Res., Sect. A **499**, 469 (2003).
[17] K. Adcox *et al.*, Phys. Rev. Lett. **86**, 3500 (2001).
[18] R. Glauber and G. Matthiae, Nucl. Phys. **B21**, 135 (1970).
[19] Woods-Saxon Au nuclear radius $R = 6.38 \pm 0.06$ fm, diffusivity $a = 0.535 \pm 0.027$ fm [B. Hahn, D. G. Ravenhall, and R. Hofstadter, Phys. Rev. **101**, 1131 (1956)], and nucleon-nucleon cross section $\sigma_{NN}^{\mathrm{inel}} = 42 \pm 3$ mb.
[20] GEANT 3.2.1, CERN program library.
[21] W. A. Zajc *et al.*, Phys. Rev. C **29**, 2173 (1984).
[22] S. Chapman, P. Scotto, and U.W. Heinz, Phys. Rev. Lett. **74**, 4400 (1995); Heavy Ion Phys. **1**, 1 (1995).
[23] P. Avery *et al.*, Phys. Rev. D **32**, 2294 (1985).
[24] M. G. Bowler, Phys. Lett. B **270**, 69 (1991).
[25] Y. M. Sinyukov, R. Lednicky, S.V. Akkelin, J. Pluta, and B. Erazmus, Phys. Lett. B **432**, 248 (1998).
[26] D. Adamova *et al.*, Nucl. Phys. **A714**, 124 (2003).
[27] U. A. Wiedemann and U. Heinz, Phys. Rev. C **56**, 3265 (1997).
[28] J. Adams *et al.*, Phys. Rev. Lett. **93**, 012301 (2004).
[29] T. Hirano and K. Tsuda, Phys. Rev. C **66**, 054905 (2002).
[30] S. Soff, hep-ph/0202240.
[31] F. Retiere and M. A. Lisa, nucl-th/0312024.
[32] M. Csanád, T. Csörgő, B. Lörstad, and A. Ster, J. Phys. G **30**, S1079 (2004).
[33] W. Broniowski, A. Baran, and W. Florkowski, AIP Conf. Proc. **660**, 185 (2003).
[34] L. Ahle *et al.*, Phys. Rev. C **66**, 054906 (2002).